World Electric Vehicle Journal

MDPI

Article

The Soft Fixed Route Hybrid Electric Aircraft Charging Problem with Variable Speed

Anthony Deschênes [1]*, Raphaël Boudreault [2], Jonathan Gaudreault [1] and Claude-Guy Quimper [2]

[1] Université Laval, 2325 Rue de l'Université, Québec, Québec, Canada, G1V 0A6; {anthony.deschenes, jonathan.gaudreault, claude-guy.quimper}@ift.ulaval.ca
[2] Thales, 1405 Boul. du Parc Technologique, Québec, Québec, Canada, G1P 4P5; raphael.boudreault@thalesgroup.com
* Correspondence: anthony.deschenes@ift.ulaval.ca

Abstract: The shift toward sustainable aviation has accelerated research into hybrid electric aircraft, particularly in the context of Regional Air Mobility. To support this transition, we introduce the Soft Fixed Route Hybrid Electric Aircraft Charging Problem with Variable Speed (S-FRHACP-VS), a novel optimization problem for managing hybrid electric aircraft operations that considers variable speed. The objective is to minimize total costs by determining charging strategies, refueling decisions, hybridization ratios, and speed decisions while adhering to a soft schedule. This paper introduces an iterative variable-based fixation heuristic, named Iterative Two-Stage Mixed-Integer Programming Heuristic (*ITS-MIP-H*), that alternatively optimizes speed and hybridization ratios while considering the soft schedule constraints and nonlinear charging and energy consumption functions. In addition, a metaheuristic genetic algorithm is proposed as an alternative optimization approach. Experiments on ten realistic flight instances demonstrate that optimizing speed leads to an average cost reduction of 7.64% compared to the best non-speed-optimized model, with reductions of up to 18.64% compared to an all-fuel-based heuristic. Although genetic algorithm provides a viable alternative that performs better than the best non-speed-optimized model, the proposed iterative variable-based fixation heuristic approach consistently outperforms the metaheuristic, achieving the best solutions within seconds. These results provide new insights into the integration of hybrid electric aircraft within transportation networks, contributing to advancements in aircraft routing optimization, energy-efficient operations, and sustainable aviation policy development.

Keywords: S-FRHACP-VS; Mixed-Integer Programming; Genetic Algorithms; Nonlinear Energy Consumption; Nonlinear Charging Function; Iterative Variable-based Fixation Heuristic; Hybrid Electric Aircraft

Received: 9 July 2025
Revised: 29 July 2025
Accepted: 7 August 2025
Published:

Citation: Deschênes, A.; Raphaël, B.; Gaudreault, J.; Quimper, CG. The Soft Fixed Route Hybrid Electric Aircraft Charging Problem with Variable Speed. *World Electr. Veh. J.* **2025**, *1*, 0. https://doi.org/

List of Abbreviations

Abbreviation	Definition
FRHACP	Fixed Route Hybrid Electric Aircraft Charging Problem
S-FRHACP	Soft FRHACP
S-FRHACP-VS	S-FRHACP with Variable Speed
FRVCP	Fixed Route Electric Vehicle Charging Problem
MIP	Mixed-Integer Programming
ITS-MIP-H	Iterative Two-Stage MIP Heuristic
ITS-MIP-H-One-It	ITS-MIP-H ran on a single iteration
S1-MIP-H	Stage-1 MIP Heuristic
GA	Genetic Algorithm
GA-Warm-Start	GA with warm start
DP	Dynamic Programming
DP+GD	Dynamic Programming with Gradient Descent Post-Treatment
FF-H	Fuel-First Heuristic
MB-H	Max-Battery Heuristic
eVTOL	Electric Vertical Takeoff and Landing
TB	Toulouse-Bordeaux
OT	Ottawa-Toronto
KT	Kelowna-Thunderbay
ST	Saint-Johns-Thompson
TV	ThunderBay-Vancouver
VT	Vancouver-Toronto

1. Introduction

Historically, air transportation has relied heavily on aircraft propelled by combustion engines that use non-renewable fossil fuels. However, in recent years, there has been a growing interest in exploring alternative propulsion systems aiming to reduce greenhouse gas emissions from aviation [1]. For that purpose, electric-powered aircraft, including hybrid electric aircraft that combine internal combustion engines with electric power sources, have been proposed. Projects such as NASA electrified Powertrain Flight Demonstration [2] and case studies on electric air taxis [3] are currently in progress exploring these promising avenues. These aircraft are expected to play a crucial role in advanced air mobility, operating in a variety of multi-flight missions, including on-demand services of varying length and duration [4].

Advanced air mobility refers to the next generation of air transportation systems designed to move people and goods efficiently using innovative aircraft technologies, such as electric vertical takeoff and landing (eVTOL) aircraft, autonomous drones, and hybrid electric propulsion systems [5]. Advanced air mobility encompasses urban air mobility, which focuses on short-range air travel within cities (e.g., air taxis), regional air mobility, which connects suburban, rural, and remote areas typically inside a country, micro air mobility focusing on good deliveries with eVTOL, typically inside a city, and intercontinental air mobility, which connects different countries. Multiple research projects focus on urban air mobility and micro air mobility, mainly for last mile delivery of goods [6–8] and taxi services using eVTOL [3]. Regional air mobility has received less interest in the context of passenger transportation, with most research done on analyzing the potential of electric or hybrid electric aircraft for this use case [9,10]. Other studies focus on the development of such aircraft [11,12], while there is a research gap on how such hybrid electric aircraft will be operated in the future of advanced air mobility. The purpose of this paper is to fill this

gap and explore the potential benefits of using such an aircraft for companies.

Recent studies on hybrid electric aircraft routing have focused mainly on fixed-speed operations, often neglecting the dynamic nature of real-world missions. For example, problems such as the Fixed Route Hybrid electric Aircraft Charging Problem (FRHACP) [13] and the extended FRHACP [14] optimize total costs under static speed assumptions, limiting the potential savings coming from variable speed that exploits the non-linearity of the energy consumption functions. Moreover, the lack of a public dataset for these problems hinders future research. These limitations underscore the need for a more comprehensive framework that integrates variable-speed decisions while providing a public dataset to support future research.

However, the adoption of electric propulsion introduces several complex challenges. Beyond flight path planning, effectively managing energy consumption throughout entire missions is critical. This includes considering aircraft specifications, infrastructure availability, security requirements, and scheduling priorities. Such considerations are particularly important from a planning point of view given the current non-negligible and nonlinear duration of electricity charging [15]. Operators must make informed decisions about refueling and charging at each mission terminal. Additionally, the consideration of hybridization introduces decisions on the energy source to use (electricity and/or fuel)—the hybridization ratio—during each flight leg. These decisions require prediction of the energy consumption from nonlinear energy models depending, among others, on vehicle characteristics, speed, mass, and temperature [16–18]. Ultimately, the main goal for operators is to minimize overall mission costs by ensuring efficient energy utilization.

In summary, the contributions of this paper are the following:

- We introduce the S-FRHACP-VS, a novel optimization problem for managing hybrid electric aircraft operations that considers variable speed;
- We propose a new iterative variable-based fixation heuristic (Iterative Two-Stage MIP Heuristic) to solve it;
- We propose a new genetic algorithm approach to solve it;
- A benchmark of ten realistic instances is published for this problem;
- The proposed approaches are compared on this benchmark with previously published approaches for similar problems.

2. Background

This paper builds upon two previously published papers [13,14]. The first [13] introduces the Fixed Route Hybrid Electric Aircraft Charging Problem (FRHACP), where we optimize the energy management of a hybrid electric aircraft for a fixed route. It is similar to the Fixed Route Electric Charging Problem (FRVCP), a subproblem of the Electric Vehicle Routing Problem introduced by Montoya *et al.* [15]. Although both problems involve optimizing energy consumption across a fixed route, FRHACP differs in four fundamental ways: 1) the vehicle is a hybrid electric aircraft, introducing hybridization ratio decisions between fuel and electricity; 2) hard scheduling constraints must be respected that can limit charging duration at terminals; 3) the energy consumption functions are significantly more complex than in FRVCP, as fuel weight changes the mass of the aircraft, affecting the energy consumption; and 4) the objective function of the FRHACP is to minimize total costs while the FRVCP minimizes total duration. Despite these differences, the approaches used to solve the FRVCP can be adapted to solve the FRHACP, such as dynamic programming [13] and Mixed-Integer Programming [14]. Moreover, similar MIP-based

optimization frameworks have been proposed in ground transportation contexts, such as tramway networks [19], where hybrid storage systems under operational constraints offer insights directly transferable to the infrastructure and scheduling challenges addressed by the S-FRHACP-VS.

The FRHACP considers hybrid electric aircraft in a multi-flight mission setting. Formally, a mission is defined as a fixed route $r := (n_1, n_2, \ldots, n_{|\mathcal{N}|})$ of consecutive *nodes* $n_i \in \mathcal{N}$. Each node $n_i \in \mathcal{N}$ on the route is either a *terminal* from set $\mathcal{T}$ or a *waypoint* from set $\mathcal{W}$ ($\mathcal{N} := \mathcal{T} \cup \mathcal{W}$). A terminal is typically an airport where facilities are available to refuel and charge the aircraft. The route r starts and ends at a terminal, n_1 and $n_{|\mathcal{N}|} \in \mathcal{T}$, while r induces a natural order $\tau_1, \tau_2, \ldots, t_{|\mathcal{T}|}$ on the terminals in $\mathcal{T}$. Between consecutive terminals, the route is defined by waypoints, typically reference points in the air that must be part of the aircraft trajectory. We define *legs* as route segments connecting two consecutive nodes such as $L := \{(n_i, n_{i+1}) : i = 1, \ldots, |\mathcal{N}| - 1\}$. The different parameters of the FRHACP are listed in Table 1.

We resume the decision variables of the FRHACP, presented in Table 2, as follows. For each terminal $\tau \in \mathcal{T}$, $F_\tau^{\mathcal{D}}$ and $S_\tau^{\mathcal{D}}$ are respectively the fuel quantity and state of charge of the aircraft when leaving terminal τ. Then, for each leg $l \in \mathcal{L}$, D_l^f is the hybridization ratio on leg l as its distance traveled using fuel. The intermediate variables $F_\tau^{\mathcal{A}}$ and $S_\tau^{\mathcal{A}}$ describe the deduced fuel quantity and state of charge upon arrival at terminal $\tau \in \mathcal{T}$, while the distance traveled using electricity, D_l^s, is deduced by $D_l^s = d_l - D_l^f \forall l \in \mathcal{L}$. The objective is to minimize fuel and electricity costs as expressed by Equation (1), with c_τ^s and c_τ^f respectively being the electricity and fuel costs at terminal τ.

$$\min \sum_{\tau \in \mathcal{T}} \left(c_\tau^s (S_\tau^{\mathcal{D}} - S_\tau^{\mathcal{A}}) + c_\tau^f (F_\tau^{\mathcal{D}} - F_\tau^{\mathcal{A}}) \right) \tag{1}$$

In our second paper [14], we introduce the Extended-FRHACP, an extension of the FRHACP where the schedule is subject to a soft constraint on arrival and departure times at each terminal with monetary costs associated with deviation from the given scheduled times. Furthermore, it adds a decision of waiting, i.e. to perform other tasks (e.g., for maintenance purposes) than charging and refueling at the charging and refueling stations at a terminal, which can be constrained. Decision variables $T_\tau^{\mathcal{A}}$ and $T_\tau^{\mathcal{D}}$ are thus added for each terminal $\tau \in \mathcal{T}$ that respectively represent the arrival and departure times at terminal τ, which can differ from the scheduled arrival and departure times ($t^{\mathcal{A}}$ and $t^{\mathcal{D}}$ respectively). Moreover, additional constraints such as maximum charging duration and fuel availability can be specified at each terminal, while the availability of charging/refueling facilities can also vary. Finally, the possibility of enforcing a specific source of energy to use on a given leg (e.g., forcing taxi phases to use electricity) is added. The objective function is expressed by Equation (2), with $c^{<t^{\mathcal{A}}}$ and $c^{>t^{\mathcal{A}}}$ being respectively the costs associated with arriving before or after the arrival scheduled time and $c^{<t^{\mathcal{D}}}$ and $c^{>t^{\mathcal{D}}}$ being respectively the costs associated with departing before or after the departure scheduled time at each terminal $\tau \in \mathcal{T}$. In this paper, we formally name this problem Soft-FRHACP (S-FRHACP).

$$\begin{aligned} \min \sum_{\tau \in \mathcal{T}} \big(& c_\tau^s (S_\tau^{\mathcal{D}} - S_\tau^{\mathcal{A}}) + c_\tau^f (F_\tau^{\mathcal{D}} - F_\tau^{\mathcal{A}}) \quad + \\ & c_\tau^{<t^{\mathcal{A}}} \max(0, t_\tau^{\mathcal{A}} - T_\tau^{\mathcal{A}}) + c_\tau^{>t^{\mathcal{A}}} \max(0, T_\tau^{\mathcal{A}} - t_\tau^{\mathcal{A}}) \quad + \\ & c_\tau^{<t^{\mathcal{D}}} \max(0, t_\tau^{\mathcal{D}} - T_\tau^{\mathcal{D}}) + c_\tau^{>t^{\mathcal{D}}} \max(0, T_\tau^{\mathcal{D}} - t_\tau^{\mathcal{D}}) \big) \end{aligned} \tag{2}$$

For the S-FRHACP [14], five approaches ranging from heuristics to exact methods are proposed to solve the problem:

- Fuel-First Heuristic (*FF-H*): This heuristic aims to maximize fuel usage. It only uses electricity when mandatory (such as the legs that are enforced on electricity). Its main goal is to be a comparison point to estimate the potential gains of using the hybrid engine.
- Max-Battery Heuristic (*MB-H*): This heuristic aims at maximizing battery usage by always consuming fuel first, and then finishing using the electricity. It is based on the assumption that, on a given leg, consuming fuel first is the optimal strategy [20]. However, this assumption is false when looking at a flight composed of a series of legs [13]. At each terminal, we charge at maximum capacity while respecting the schedule and other constraints such as limited charging duration, then take the smallest amount of fuel in order to complete the flight.
- Dynamic Programming (*DP*): This heuristic uses dynamic programming to minimize fuel consumption for all flights. Based on different mostly realistic assumptions, such that fuel costs are higher than electricity costs and that fuel costs are the same at each terminal, it has been shown to be the optimal strategy to optimize total costs for the FRHACP [13], while producing good solutions for the S-FRHACP [14].
- Dynamic Programming with Gradient Descent Post-Treatment (*DP+GD*): This heuristic is the same as *DP*, where a gradient descent post-treatment is applied to handle cases where fuel cost varies between terminals. It has been shown to yield optimal results for the FRHACP [13] and good results for the S-FRHACP [14].
- Mixed-Integer Programming (MIP): This MIP model solves the S-FRHACP to optimality with respect to its approximations of the energy consumption function and the charging duration functions [14]. It is the state-of-the-art for the S-FRHACP, obtaining optimal solutions within seconds on a benchmark of ten realistic instances. In this paper, this model is used as a comparison point as the best approach that does not optimize speed.

Experiments were conducted on a benchmark of 10 realistic instances, described in detail in Section 3.4, with realistic schedule, fuel and electricity costs, and flight itineraries. The results show that the MIP model reduces total costs on average by 15% compared to the *FF-H*, with a solving time on average below 10 seconds. Scalability analysis demonstrates that the MIP model can solve in reasonable time instances of up to 15 terminals, while realistic instances do not exceed 10 terminals.

3. Materials and Methods

3.1. Problem Definition: The Soft Fixed Route Hybrid Electric Aircraft Charging Problem with Variable Speed (S-FRHACP-VS)

The S-FRHACP-VS is a generalization of the S-FRHACP where flight speed decisions are added. It asks to decide how much to refuel and charge the aircraft at each terminal while deciding the hybridization ratio and flight speed for each leg. These decisions are limited by security margins, physical capacity, and soft schedule constraints on departure and arrival times. The time required to charge the aircraft battery at a terminal is encoded as a function dependent on the initial and final states of charge, usually nonlinear [15], while the refueling duration is given by a constant rate. Hybridization ratio decisions on the energy source to use (electricity and/or fuel) during each leg are encoded as the traveled distance using fuel first. This is based on the hypothesis that fuel has a non-negligible mass, which is an important nonlinear factor in energy consumption prediction [16–18], and that using fuel first is the optimal energy management strategy on a leg [20]. Thus, fuel and electricity consumption models are encoded as functions dependent on the traveled

distance, the total mass, and the flight speed. These may include other physical parameters, such as altitude, and trajectory angle, but are assumed constant on a given leg (but can vary between legs). Moreover, monetary costs are associated to the deviation from the given scheduled times. It is thus possible to *wait* at a terminal, i.e. to perform other tasks than charging and refueling at a terminal, which can be constrained (e.g., for maintenance purposes). A maximal charging duration and fuel availability can be specified as constraints at each terminal, while the availability of charging/refueling facilities can also vary. Finally, a specific source of energy to use can be enforced on a given leg (e.g., to enforce that taxi phases use electricity). Figure 1 presents a visual representation of an instance of the S-FRHACP-VS and the different decision variables related to the problem. In summary, an S-FRHACP-VS instance requires the parameters listed in Table 1 and the decision variables are listed in Table 2. Elements are split between the elements specific for the FRHACP, the S-FRHACP, and the S-FRHACP-VS. These tables are additives, such that the S-FRHACP uses all elements from the FRHACP in addition to the listed ones, while the S-FRHACP-VS uses all elements. Finally, the objective of the S-FRHACP-VS is the same as for the S-FRHACP, i.e., to minimize total costs, as expressed by Equation (2).

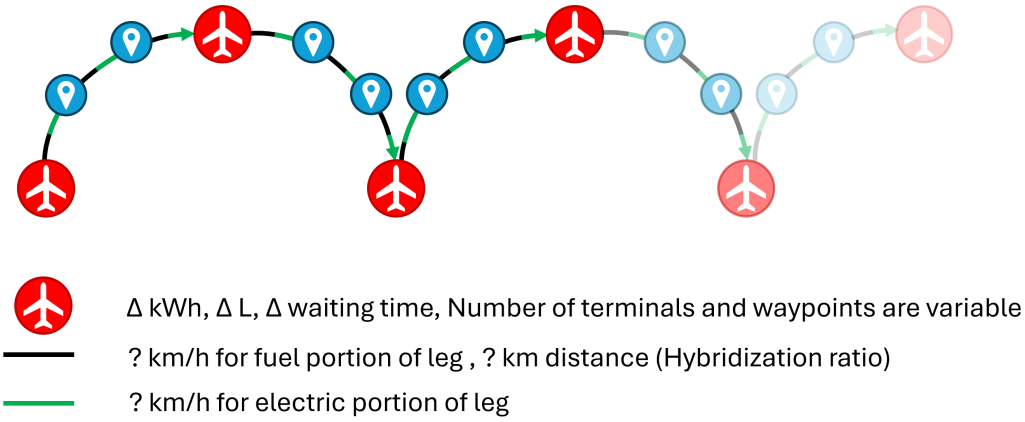

Figure 1. Visual representation of an instance of the S-FRHACP-VS and its decision variables. The fixed route is composed of a series of terminals (typically airports) with waypoints splitting the route between two terminals. The decision variables are split between terminal's decisions (charging quantity, refueling quantity, and waiting time) and leg's decisions (flight speed on the fuel and electric portion of the leg, and hybridization ratio).

3.1.1. Challenges for optimizing speed

Solving the S-FRHACP-VS requires to consider the speed on each leg when using electricity and fuel. Since the constraints encoding the duration divide the distance by speed, direct optimization of speed within a MIP model is impractical. Therefore, optimizing the duration of the route becomes the only feasible option (since duration encodes speed). As a result, the nonlinear energy consumption functions on each leg are functions of three decision variables: 1) the distance, equivalent to the hybridization ratio decisions; 2) the weight, affected by the fuel taken on the previous terminals and the hybridization ratio decisions; and 3) the route duration, which is dependent on the speed and distance. While Misener *et al.* [21] describe methods to encode such functions in a MIP model, the extensive sampling required for accurate approximations slows the MIP model excessively. Additionally, distance and route duration are interdependent, complicating sampling: some combinations of these variables are infeasible, and introducing infinity in the sampling fails to handle these cases properly. As a result, designing an exact MIP model to solve the

Table 1. Description of the different parameters required by an instance of the S-FRHACP-VS, with their unit, split between the specific parameters for the FRHACP, the S-FRHACP, and the S-FRHACP-VS.

Parameter	Description	Unit
	FRHACP	
s_1	Initial state of charge at the origin	%
f_1	Initial fuel quantity at the origin	L
t_1	Initial time at the origin	h
$s^{\min}$	Minimal state of charge	%
$s^{\max}$	Maximal state of charge	%
$f^{\min}$	Minimal fuel quantity	L
$f^{\max}$	Maximal fuel quantity	L
$t_\tau^{\mathcal{D}}$	Scheduled departure time at terminal $\tau \in \mathcal{T}$	h
α^f	Refueling rate of the aircraft	L/h
m^f	Fuel mass	kg/L
m^a	Empty aircraft mass	kg
m_l^p	Payload mass on leg $l \in \mathcal{L}$	kg
d_l	Travel distance on leg $l \in \mathcal{L}$	km
v_l	Recommended aircraft speed on leg $l \in \mathcal{L}$	km/h
$\delta_l^s(d, m, v)$	Function of the electricity consumption given the distance d (km), the mass m (kg), and the speed v (km/h) on leg $l \in \mathcal{L}$	%
$\delta_l^f(d, m, v)$	Function of the fuel consumption given the distance d (km), the mass m (kg), and the speed v (km/h)d on leg $l \in \mathcal{L}$	L
c_τ^s	Electricity cost at terminal $\tau \in \mathcal{T}$	\$/%
c_τ^f	Fuel cost at terminal $\tau \in \mathcal{T}$	\$/L
	S-FRHACP	
$t_\tau^{\mathcal{A}}$	Scheduled arrival time at terminal $\tau \in \mathcal{T}$	h
$\Delta t_\tau^{\text{wait,min}}$	Minimal waiting duration at terminal $\tau \in \mathcal{T}$	h
$\Delta t_\tau^{s,\max}$	Maximal charging duration at terminal $\tau \in \mathcal{T}$	h
$\Delta f_\tau^{\max}$	Available fuel quantity at terminal $\tau \in \mathcal{T}$	L
can_τ^s	1 if we can charge at terminal $\tau \in \mathcal{T}$, else 0	Bool
can_τ^f	1 if we can refuel at terminal $\tau \in \mathcal{T}$, else 0	Bool
allowed_l^s	1 if we can use electricity on leg $l \in \mathcal{L}$, else 0	Bool
allowed_l^f	1 if we can use fuel on leg $l \in \mathcal{L}$, else 0	Bool
$c_\tau^{<t^{\mathcal{A}}}$	Cost of arriving earlier than the scheduled arrival time at terminal $\tau \in \mathcal{T}$	\$/h
$c_\tau^{>t^{\mathcal{A}}}$	Cost of arriving later than the scheduled arrival time at terminal $\tau \in \mathcal{T}$	\$/h
$c_\tau^{<t^{\mathcal{D}}}$	Cost of departing earlier than the scheduled departure time at terminal $\tau \in \mathcal{T}$	\$/h
$c_\tau^{>t^{\mathcal{D}}}$	Cost of departing later than the scheduled departure time at terminal $\tau \in \mathcal{T}$	\$/h
	S-FRHACP-VS	
$v_l^{\min}$	Minimal speed on leg $l \in \mathcal{L}$	km/h
$v_l^{\max}$	Maximal speed on leg $l \in \mathcal{L}$	km/h

S-FRHACP-VS remains challenging. Thus, in this paper, we propose two new heuristics to solve this problem. One is based on an iterative variable-based fixation heuristic, inspired by Wilbaut *et al.* [22] and described in Section 3.2, while the other is based on genetic algorithm, described in Section 3.3.

Table 2. Decision variables of the S-FRHACP-VS, with their domain and unit, split between the specific variables for the FRHACP, the S-FRHACP, and the S-FRHACP-VS.

Variable	Domain	Description	Unit
		FRHACP	
$S_n^{\mathcal{A}}$	$[s^{\min}, s^{\max}]$	Arrival state of charge at node $n \in \mathcal{N}$	%
$S_n^{\mathcal{D}}$	$[s^{\min}, s^{\max}]$	Departure state of charge at node $n \in \mathcal{N}$	%
$F_n^{\mathcal{A}}$	$[f^{\min}, f^{\max}]$	Arrival fuel quantity at node $n \in \mathcal{N}$	L
$F_n^{\mathcal{D}}$	$[f^{\min}, f^{\max}]$	Departure fuel quantity at node $n \in \mathcal{N}$	L
D_l^s	$[0, d_l]$	Traveled distance using electricity on leg $l \in \mathcal{L}$	km
D_l^f	$[0, d_l]$	Traveled distance using fuel on leg $l \in \mathcal{L}$	km
		S-FRHACP	
$\Delta T_\tau^{\text{wait}}$	$[\Delta t_\tau^{\text{wait,min}}, \infty]$	Waiting duration at terminal $\tau \in \mathcal{T}$	h
		S-FRHACP-VS	
V_l^s	$[v_l^{\min}, v_l^{\max}]$	Aircraft speed using electricity on leg $l \in \mathcal{L}$	km/h
V_l^f	$[v_l^{\min}, v_l^{\max}]$	Aircraft speed using fuel on leg $l \in \mathcal{L}$	km/h

3.2. Solving the S-FRHACP-VS: Iterative Two-Stage Mixed-Integer Programming Heuristic (ITS-MIP-H)

We propose an iterative variable-based fixation heuristic, named the Iterative Two-Stage MIP heuristic (*ITS-MIP-H*), to solve the S-FRHACP-VS. It solves the problem of interdependency between the duration and distance by solving them in two separate Stages. In the first Stage, the S-FRHACP (without variable speed) is optimized using the MIP model of Deschênes *et al.* [14] (*S1-MIP-H*), which assumes a constant speed—initially the recommended speed, and, in subsequent iterations, the speed obtained from Stage 2. In the second Stage, a different MIP model described in Section 3.2.1 is used to address varying speed, where the distances are fixed at the optimal values found in Stage 1. As a result, each MIP model applies perturbations on the instance of the next MIP model, allowing to escape local minima. This process can then be repeated until convergence, perturbing alternatively the speeds and distances of each instance of the MIP models. By fixing speeds and distances alternatively, the complexity of the Stage-2 MIP model is similar to the complexity of the Stage-1 MIP model for the S-FRHACP. Figure 2 presents a visual representation of the *ITS-MIP-H*. This heuristic is guaranteed to converge since at each Stage we can either improve the total costs or select the optimal speeds or distances that are the same as for the previous Stage. This is used as a stopping criterion, i.e., when the solution does not change between two consecutive iterations. However, it is not guaranteed that the *ITS-MIP-H* converges to a global optimum.

3.2.1. Stage-2 MIP model

The Stage-2 MIP model considers that the hybridization ratio decisions are parameters (instead of decision variables) and optimizes the duration of the legs on fuel and on electricity. Once the distances are fixed, deciding the duration is equivalent to deciding the speed. The model is similar to the MIP model of Deschênes *et al.* [14]. The main differences are: 1) traveled distance variables are now fixed parameters; 2) the speed on each leg is encoded as the duration traveled using fuel or electricity, thus transforming some constraints in decision variables; and 3) the energy consumption functions are dependent on the weight and the duration of the leg (instead of the weight and the distance). As a result, a new hyperparameter is introduced, the number of points in the grid for the duration, $\tilde{t}$, used to

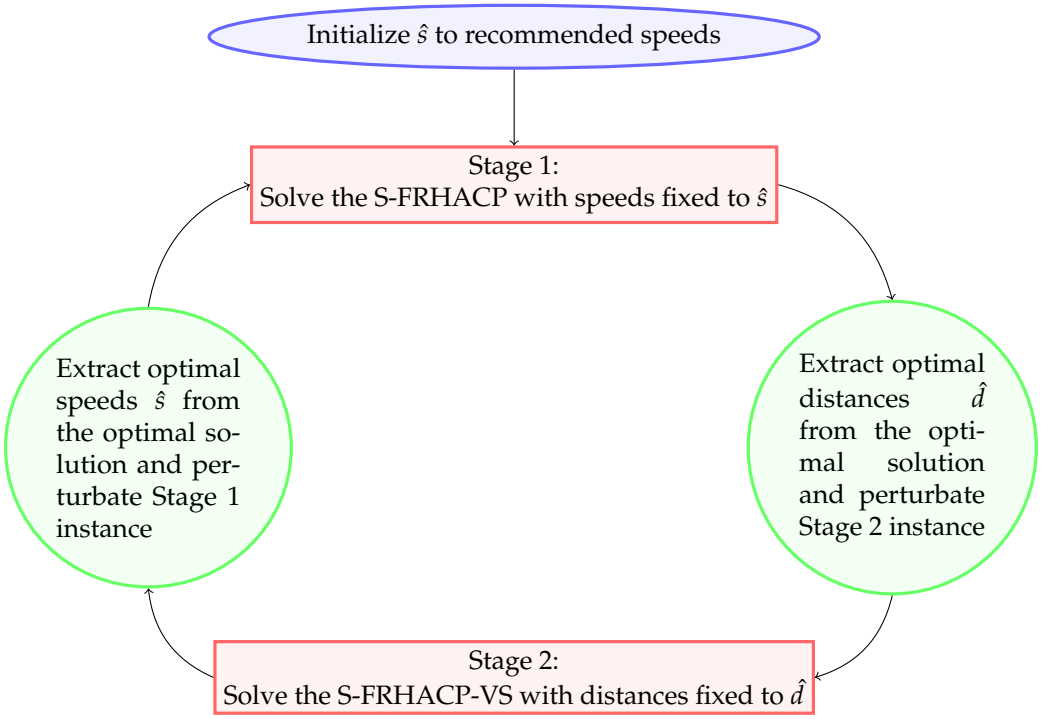

Figure 2. Flowchart representing the Iterative Two-Stage MIP Heuristic for the S-FRHACP-VS. The heuristic starts by fixing the speeds to the initial recommended speeds, then solve the resulting S-FRHACP instance in Stage 1. The optimal distances are extracted from the optimal solution of Stage 1. Then, the heuristic solves the S-FRHACP-VS where the distances are fixed to the extracted distances (using the Stage-2 MIP model). Finally, the optimal speeds are extracted from the optimal solution of the Stage 2 and the process can then be repeated using the newly extracted speeds until convergence.

linearize the energy consumption functions.

Variables

As for the S-FRHACP, the main decision variables for the Stage-2 MIP model of the S-FRHACP-VS are related to the charging and refueling durations/quantities, and the waiting duration at each terminal. Moreover, speed decisions are encoded as the duration on electricity or fuel on each leg. These variables, as well as the intermediate variables used by the MIP model, are presented in Table 3, along with their initial domain based on the parameters from Table 1.

Objective

The objective is to minimize the total cost of the multi-flight mission. It includes energy-related costs (charging and refueling), as in the S-FRHACP, but also costs induced by deviation from the scheduled arrival and departure times. It is the equivalent to Equation (2), with intermediate variables representing the costs of the deviation of the schedule.

$$\min \sum_{\tau \in \mathcal{T}} \left[c^s_\tau (S^{\mathcal{D}}_\tau - S^{\mathcal{A}}_\tau) + c^f_\tau (F^{\mathcal{D}}_\tau - F^{\mathcal{A}}_\tau) + C^{<t^{\mathcal{A}}}_\tau + C^{>t^{\mathcal{A}}}_\tau + C^{<t^{\mathcal{D}}}_\tau + C^{>t^{\mathcal{D}}}_\tau \right]$$

Table 3. Variables of the Stage-2 MIP model and their initial domain.

Variable	Domain	Description	Unit
ΔT_τ^s	$[0, \Delta t_\tau^{s,\max}]$	Charging duration at terminal $\tau \in \mathcal{T}$	h
ΔT_τ^f	$[0, \frac{1}{\alpha^f} \cdot \Delta f_\tau^{\max}]$	Refueling duration at terminal $\tau \in \mathcal{T}$	h
$\Delta T_\tau^{\text{wait}}$	$[\Delta t_\tau^{\text{wait,min}}, \infty]$	Waiting duration at terminal $\tau \in \mathcal{T}$	h
$S_n^{\mathcal{A}}$	$[s^{\min}, s^{\max}]$	Arrival state of charge at node $n \in \mathcal{N}$	%
$S_n^{\mathcal{D}}$	$[s^{\min}, s^{\max}]$	Departure state of charge at node $n \in \mathcal{N}$	%
$F_n^{\mathcal{A}}$	$[f^{\min}, f^{\max}]$	Arrival fuel quantity at node $n \in \mathcal{N}$	L
$F_n^{\mathcal{D}}$	$[f^{\min}, f^{\max}]$	Departure fuel quantity at node $n \in \mathcal{N}$	L
M_l^s	$[m^a, \infty]$	Mass of the aircraft when using electricity on leg $l \in \mathcal{L}$	kg
M_l^f	$[m^a, \infty]$	Mass of the aircraft when using fuel on leg $l \in \mathcal{L}$	kg
ΔT_l^s	$[0, d_l / v_l^{\min}]$	Traveled duration using electricity on leg $l \in \mathcal{L}$	h
ΔT_l^f	$[0, d_l / v_l^{\min}]$	Traveled duration using fuel on leg $l \in \mathcal{L}$	h
$T_n^{\mathcal{A}}$	$[t_1, \infty]$	Arrival time at node $n \in \mathcal{N}$	h
$T_n^{\mathcal{D}}$	$[t_1, \infty]$	Departure time at node $n \in \mathcal{N}$	h
$C_\tau^{<t^{\mathcal{A}}}$	$[0, \infty]$	Total cost for arriving early at terminal $\tau \in \mathcal{T}$	$
$C_\tau^{>t^{\mathcal{A}}}$	$[0, \infty]$	Total cost for arriving late at terminal $\tau \in \mathcal{T}$	$
$C_\tau^{<t^{\mathcal{D}}}$	$[0, \infty]$	Total cost for departing early at terminal $\tau \in \mathcal{T}$	$
$C_\tau^{>t^{\mathcal{D}}}$	$[0, \infty]$	Total cost for departing late at terminal $\tau \in \mathcal{T}$	$

Constraints

The constraints of the Stage-2 MIP model are presented below. We use M as a sufficiently large constant. Constraints (3) set the initial conditions at $n_1 \in \mathcal{T}$.

$$S_{n_1}^{\mathcal{A}} = s_1,\ F_{n_1}^{\mathcal{A}} = f_1,\ T_{n_1}^{\mathcal{A}} = t_1 \tag{3}$$

Constraints (4) ensure that the charging duration is a function of the arrival and departure state of charges at a terminal. This function is usually nonlinear and must be linearized in the model. Constraints (5) ensure that charging is only possible when allowed. Similarly, constraints (6) ensure that the refueling duration at a terminal is proportional to the aircraft refueling rate, while constraints (7) allow refueling only when allowed.

$$\Delta T_\tau^s = \boldsymbol{\alpha}_{\boldsymbol{\tau}}^{\boldsymbol{s}}(S_\tau^{\mathcal{A}}, S_\tau^{\mathcal{D}}) \qquad \forall \tau \in \mathcal{T} \tag{4}$$

$$\Delta T_\tau^s \leq M \cdot \text{can}_\tau^s \qquad \forall \tau \in \mathcal{T} \tag{5}$$

$$\Delta T_\tau^f = \frac{1}{\alpha^f}(F_\tau^{\mathcal{D}} - F_\tau^{\mathcal{A}}) \qquad \forall \tau \in \mathcal{T} \tag{6}$$

$$\Delta T_\tau^f \leq M \cdot \text{can}_\tau^f \qquad \forall \tau \in \mathcal{T} \tag{7}$$

By assumption, constraints (8) enforce that charging, refueling, and waiting are not allowed at any waypoint.

$$S_w^{\mathcal{D}} = S_w^{\mathcal{A}},\quad F_w^{\mathcal{D}} = F_w^{\mathcal{A}},\quad T_w^{\mathcal{D}} = T_w^{\mathcal{A}} \qquad \forall w \in \mathcal{W} \tag{8}$$

Constraints (9) define the mass of the aircraft at the beginning of each leg based on its initial fuel quantity. Since fuel consumption reduces the mass of the aircraft, constraints (10) calculate the mass of the aircraft during the electric part of the leg after considering the fuel used on the fuel part of the leg. This mass can vary depending on the amount of remaining fuel, including any additional reserves kept for later use.

$$M^f_{l_i} = m^a + m^p_{l_i} + m^f F^{\mathcal{D}}_{n_i} \qquad \forall l_i := (n_i, n_{i+1}) \in \mathcal{L} \tag{9}$$

$$M^s_{l_i} = m^a + m^p_{l_i} + m^f F^{\mathcal{A}}_{n_{i+1}} \qquad \forall l_i := (n_i, n_{i+1}) \in \mathcal{L} \tag{10}$$

Constraints (11) and (12) compute the arrival state of charge and fuel at each node with respect to the energy consumption functions. These functions are nonlinear and require linearization in order to be used in the MIP model. $\hat{d}_{l_i}$ is the optimal hybridization ratio found by the Stage-1 MIP model.

$$S^{\mathcal{A}}_{n_{i+1}} = S^{\mathcal{D}}_{n_i} - \boldsymbol{\delta^s_{l_i}}(d_{l_i} - \hat{d}_{l_i}, M^s_{l_i}, (d_{l_i} - \hat{d}_{l_i})/\Delta T^s_{l_i}), \qquad \forall l_i := (n_i, n_{i+1}) \in \mathcal{L} \tag{11}$$

$$F^{\mathcal{A}}_{n_{i+1}} = F^{\mathcal{D}}_{n_i} - \boldsymbol{\delta^f_{l_i}}(\hat{d}_{l_i}, M^f_{l_i}, \hat{d}_{l_i}/\Delta T^f_{l_i}) \qquad \forall l_i := (n_i, n_{i+1}) \in \mathcal{L} \tag{12}$$

Constraints (13) encode the departure time from a terminal, defined by its arrival time, the charging and refueling durations, and the waiting duration. Constraints (14) encode the arrival time at a node according to its incoming leg duration.

$$T^{\mathcal{D}}_\tau = T^{\mathcal{A}}_\tau + \Delta T^s_\tau + \Delta T^f_\tau + \Delta T^{\text{wait}}_\tau \qquad \forall \tau \in \mathcal{T} \tag{13}$$

$$T^{\mathcal{A}}_{n_{i+1}} = T^{\mathcal{D}}_{n_i} + \Delta T^s_{l_i} + \Delta T^f_{l_i} \qquad \forall l_i := (n_i, n_{i+1}) \in \mathcal{L} \tag{14}$$

Finally, the constraints (15) to (18) relate the schedule costs to their associated time variable.

$$C^{<t^{\mathcal{A}}}_\tau \geq c^{<t^{\mathcal{A}}}_\tau (t^{\mathcal{A}}_\tau - T^{\mathcal{A}}_\tau) \qquad \forall \tau \in \mathcal{T} \tag{15}$$

$$C^{>t^{\mathcal{A}}}_\tau \geq c^{>t^{\mathcal{A}}}_\tau (T^{\mathcal{A}}_\tau - t^{\mathcal{A}}_\tau) \qquad \forall \tau \in \mathcal{T} \tag{16}$$

$$C^{<t^{\mathcal{D}}}_\tau \geq c^{<t^{\mathcal{D}}}_\tau (t^{\mathcal{D}}_\tau - T^{\mathcal{D}}_\tau) \qquad \forall \tau \in \mathcal{T} \tag{17}$$

$$C^{>t^{\mathcal{D}}}_\tau \geq c^{>t^{\mathcal{D}}}_\tau (T^{\mathcal{D}}_\tau - t^{\mathcal{D}}_\tau) \qquad \forall \tau \in \mathcal{T} \tag{18}$$

Function Linearizations

As for Deschênes *et al.* [23], the nonlinear charging functions $\boldsymbol{\alpha^s_\tau}(s_1, s_2)$ are approximated using multiple linear functions, each adding a binary variable to the model for each terminal $\tau \in \mathcal{T}$. The nonlinear electricity and fuel consumption functions, $\boldsymbol{\delta^s_l}(d, t)$ and $\boldsymbol{\delta^f_l}(d, t)$, both depend on distance and duration decisions. We approximate these multidimensional functions in the MIP model using the methodology of Misener *et al.* [21], which uses grid sampling. This leads to two hyperparameters: the number of points in the grid for the dimension of mass $\tilde{m}$ and for the dimension of duration $\tilde{t}$. The approximation adds $\tilde{m} + \tilde{t}$ binary variables for each leg $l \in \mathcal{L}$. It is known that the finer the grid, the better approximations will be, but the harder it will be to solve.

3.3. Solving the S-FRHACP-VS: Genetic Algorithm

The Iterative Two-Stage MIP Heuristic relies on approximations of the energy consumption and charging duration functions, which can affect the quality of the solution depending on the sampling size. Although these approximations can be made more precise with sufficient sampling points, the iterative nature of the two-stage heuristic also affects the returned solution. Since the model alternates between optimizing speed and hybridization ratio instead of solving them jointly, the resulting solution depends on the iterative sequence rather than converging to a guaranteed global optimum. As a result, the Iterative Two-Stage MIP Heuristic is an advanced heuristic rather than a strictly exact approach, which justifies exploring metaheuristic approaches such as genetic algorithms.

Although these approaches do not guarantee global optimality, they offer flexibility in navigating complex solution spaces and efficiently identifying high-quality solutions. Moreover, genetic algorithms are easier to implement and can directly use the nonlinear energy consumption and charging functions, making them an attractive alternative, particularly when using complex nonlinear functions such as neural networks. Since the solution space is large (approximately 200 variables), genetic algorithm is preferred over particle swarm optimization since it is known that particle swarm optimization performs poorly for high-dimensional problems [24].

3.3.1. Genes

All decision variables of the S-FRHACP-VS can be encoded using continuous variables between 0 and 1. For a given instance, the genes of an individual are sequential from n_1 to $n_{|\mathcal{N}|-1}$, as shown by Figure 3. All nodes $n_i \in \mathcal{N}$ have three genes: 1) the percentage of the traveled distance to do on fuel for the next leg (hybridization ratio); 2) the flight speed for the fuel portion of the next leg, with 0 equal to the minimum speed ($v_{l_i}^{\min}$) and 1 equal to the maximum speed ($v_{l_i}^{\max}$); and 3) the flight speed for the electric portion of the next leg with 0 equal to the minimum speed ($v_{l_i}^{\min}$) and 1 equal to the maximum speed ($v_{l_i}^{\max}$). Moreover, there are three additional genes if n_i is a terminal (these correspond to charging/refueling decisions): 1) the departure fuel quantity, with 0 equal to the minimal fuel quantity ($f^{\min}$) and 1 equal to the maximal fuel quantity ($f^{\max}$); 2) the departure state of charge, with 0 equal to the minimal state of charge ($s^{\min}$) and 1 equal to the maximum state of charge ($s^{\max}$); and 3) the waiting duration, with 0 equal to no waiting and 1 equal to the scheduled waiting duration if we respect the schedule. When n_i is a terminal, the associated genes are located before the node genes in the individual. All other intermediate variables, such as the arrival fuel and state of charge, can be determined from these variables.

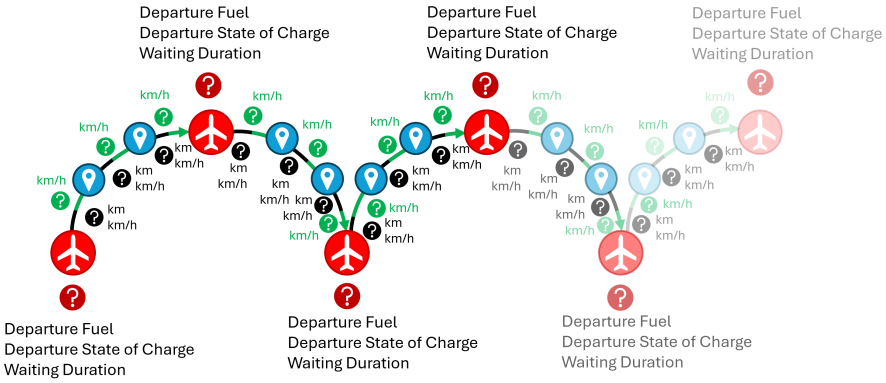

Figure 3. Visual representation of how the genetic algorithm genes relate to an instance of the S-FRHACP-VS. The first variables are at the starting terminal and they represent charging, refueling and waiting decisions. During the flights, the genes represent the hybridization ratio (km), the chosen flight speed for the fuel portion of the leg and the flight speed electric portion of the leg.

3.3.2. Fitness Function

We use a simulation to compute the total costs associated to an individual's genes. The fitness function is thus equal to Equation (2) plus a penalization function that applies an additional cost when arriving below margins for the fuel (10$/L.) and/or the state of charge (10$/%) at each terminal. These values are large enough to ensure that the best individuals respect the margins while not penalizing too much individuals that are close to respecting the margins. This penalty function is mandatory, as there is no guarantee that an individual respects these constraints. In contrast, constraints such as charging/refueling

station availability and enforcing electricity or fuel on a leg are enforced before simulating the individual by changing the value of the corresponding genes to either 0 or 1 depending on the case.

3.3.3. Warm Start

In the traditional genetic algorithm framework, the initial population is randomly sampled. However, it is also possible to provide some individuals of the initial population to guide the search. As such, we test whether giving all of the non-MIP solutions (*DP*, *DP+GD*, *FF-H*, *MB-H*) as part of the initial population helps to improve the performance of the genetic algorithm. We excluded the MIP solutions, as they can take a long time to compute, which could significantly increase the computation time of the genetic algorithm.

3.4. Experiments

We implemented the MIP models from Section 3.2 in the MiniZinc 2.9.2 language [25] and used CPLEX 22.1.2 for solving, with an optimal relative gap setting of $1e{-}10$ and a timeout of five minutes. The *DP*, its gradient descent post-treatment (*DP+GD*), and the heuristics (*FF-H*, *MB-H*) from Deschênes *et al.* [14] were also implemented in Python 3.11. The genetic algorithms were implemented in Python 3.11 using PyGAD [26]. Moreover, the optimal hybridization ratios previously found using a grid search for *DP* and *DP+GD* are now found using Brent's algorithm [27]. The experiments were performed on an Intel CoreTM Ultra 7 155H, 3800 Mhz, 16 cores, 22 logical processors, 16GB RAM. In order to compare each method on the same basis, a simulation using the non-approximated functions is always performed as a post-treatment. Additionally, all MIP models perform energy quantity corrections after the simulation to reduce their approximation errors and stay as close to their original optimal solution as possible.

3.4.1. Dataset

Our dataset consists of the ten real-life inspired instances from Deschênes *et al.* [14], which were created from day-long sequences of commercial aircraft flights in Canada and France. The dataset is available and published as a benchmark for this problem[1]. It is summarized in Table 4. All costs are presented in CAD ($). The number of terminal varies from 4 to 10, with a number of waypoints between 30 and 107, and a traveled distance of up to 9456 km.

Table 4. Description of the ten instances forming the dataset including the number of terminal ($|\mathcal{T}|$), the number of waypoints ($|\mathcal{W}|$), the total duration and distance of the combined flights, the electricity costs range (c^s) and the fuel cost range (c^f) of each instance.

Instance	$\lvert\mathcal{T}\rvert$	$\lvert\mathcal{W}\rvert$	Duration	Distance (km)	c^s ($/kWh)	c^f ($/L)
PN	4	59	4h30	2740	0.1397	1.46
TB	5	42	6h42	2812	0.1397	1.46
MS	6	30	7h22	2294	0.0533	[1.16, 1.25]
OT	7	43	9h34	4709	[0.0533, 0.1140]	[1.03, 1.28]
KT	7	47	10h45	5165	[0.0776, 0.1408]	[1.13, 1.38]
ST	6	52	13h10	6788	[0.0898, 0.1234]	[1.03, 1.37]
TV	6	64	14h36	8493	[0.0976, 0.1408]	[1.13, 1.44]
SK	7	107	16h33	9456	[0.0533, 0.1408]	[1.16, 1.44]
BK	10	72	16h46	8143	[0.0590, 0.1408]	[1.13, 1.44]
VT	5	49	11h17	5886	[0.0776, 0.1408]	[1.26, 1.41]

[1] The dataset is available at https://github.com/AnthonyDeschenes/S-FRHACP-VS-Dataset

All instances also use *Cessna S550 Citation II* as the aircraft, which is augmented with a battery of 216 kWh, and has the specifications from Deschênes *et al.* [13]. It relies on the OpenAP aircraft performance model [18] to predict energy consumption as nonlinear functions $\delta_l^s(d, m, v)$ and $\delta_l^f(d, m, v)$, using the fixed parameters of leg $l \in \mathcal{L}$. Since OpenAP does not handle consumption predictions while taxiing, we enforce that the associated legs are fully electric and instead use a physical model for electric vehicles [17]. For the charging functions $\boldsymbol{\alpha}_\tau^s(s_i, s_f)$, it uses for all terminals $\tau \in \mathcal{T}$ the nonlinear charging function from Deschênes *et al.* [23].

Additionally, we assume the following parameters for the S-FRHACP as for Deschênes *et al.* [14]. We fix the scheduled arrival times using the departure times and the planned durations. The soft schedule costs are fixed for all terminals $\tau \in \mathcal{T}$ to $c_\tau^{<t^A} = \$0.25/\text{min}$ and $c_\tau^{>t^A} = \$20/\text{min}$. Some terminals do not have electric charging stations, while every taxi leg is forced to be traveled using only electricity. For the S-FRHACP-VS, we set the maximal speed ($v_l^{\max}$) to 1.2 multiplied by the recommended speed (v_l) and the minimal speed ($v_l^{\min}$) to 0.8 multiplied by the recommended speed. For this benchmark, the remaining parameters are set in a way that does not incur additional constraints.

3.4.2. Hyperparameters Selection Methodology

Both the MIP models and DP have hyperparameters, which affect the solving time and the quality of the solution, that must be chosen. To avoid biased conclusions when comparing the approaches, these hyperparameters should be selected using an objective methodology. Following the methodology of Deschênes *et al.* [14], the dataset is split into a training set, used to determine the hyperparameters, and a test set, used to compute the results. We use the same split as for Deschênes *et al.* [14], with the training set being `PN`, `MS`, `SK`, and `BK`. The test set contains the remaining six instances. Since we use the same training and test sets as for Deschênes *et al.* [14], we use the same hyperparameters as they found for the Stage-1 MIP model, $(\tilde{d}, \tilde{m}) = (2, 4)$. For *DP* and the Stage-2 MIP model, a Pareto front of different combinations of hyperparameters is computed on the training set and the distance from the ideal point algorithm [28] is used to decide which combination of hyperparameters to use on the test set.

For the *DP* and *DP+GD* approaches, we use the same hyperparameters for both since *DP+GD* is a post-treatment of *DP*. These approaches both have two hyperparameters: $\tilde{s}$, the number of states of charge sampled by the dynamic programming algorithm, and $\tilde{d}$, the maximal number of iterations of Brent's algorithm [27] when finding the best hybridization ratio, as presented in Deschênes *et al.* [13]. For $\tilde{s}$, we tested values ranging from 10 to 100 with a step of 10. For $\tilde{d}$, we tested the following values, $[5, 6, 7, 8, 9, 10, 15, 20, 30, 40]$, for a total of 100 combinations. The values for $\tilde{d}$ are smaller than those tested by Deschênes *et al.* [14] since Brent's algorithm [27] converges quickly and takes on average 10 steps to find the optimal hybridization ratio for our training instances. Figure 4 presents the resulting Pareto front. The chosen combination of hyperparameters is point **G**, with ($\tilde{s}$, $\tilde{d}$) = (10, 15).

For the Stage-2 MIP model, the model has two hyperparameters: $\tilde{m}$ and $\tilde{t}$. These represent respectively the number of points in the grid sampling used to approximate the energy consumption functions for the weights and for the durations. Since $\tilde{m}$ has already been chosen for the Stage-1 MIP model, we also use the value of 4 for this hyperparameter in the Stage-2 MIP model. This ensures convergence when alternating between the two MIP models during the iterative process. As a result, the only hyperparameter to decide for the Stage-2 MIP model is $\tilde{t}$, which we computed values from 3 to 10 with an increment of 1 for

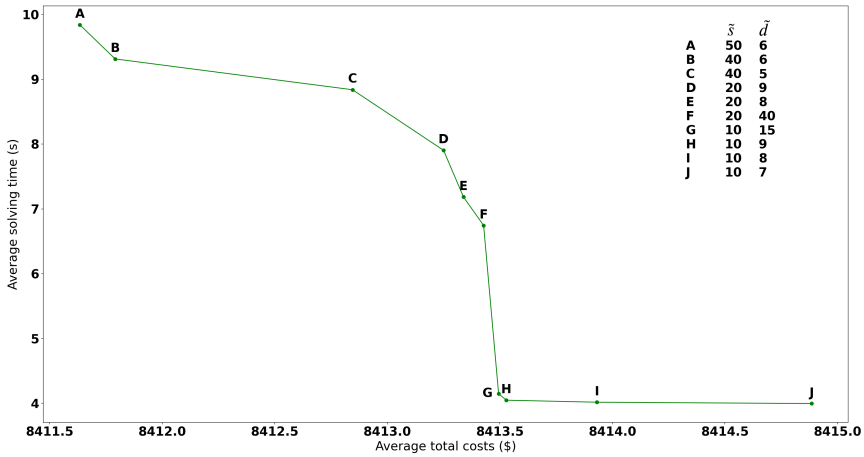

Figure 4. Resulting Pareto front for the *DP* and *DP+GD* approaches on the training set with tested hyperparameter combinations. Each point from A to J represents a combination of state of charge sampled ($\tilde{s}$) and maximal number of iterations of Brent's algorithm ($\tilde{d}$) that dominates either on average total costs or average solving time on the training set. This Pareto front can then be used to choose a combination of hyperparameters to use on the test set (Point **G**).

a total of 8 combinations. The value of 2 is not considered, since it leads to arrival states of charge below the margin due to its poor approximation of the electricity consumption function. Figure 5 presents the resulting Pareto front and the corresponding value of the hyperparameter on top of each point. The chosen hyperparameter is thus 3 for $\tilde{t}$.

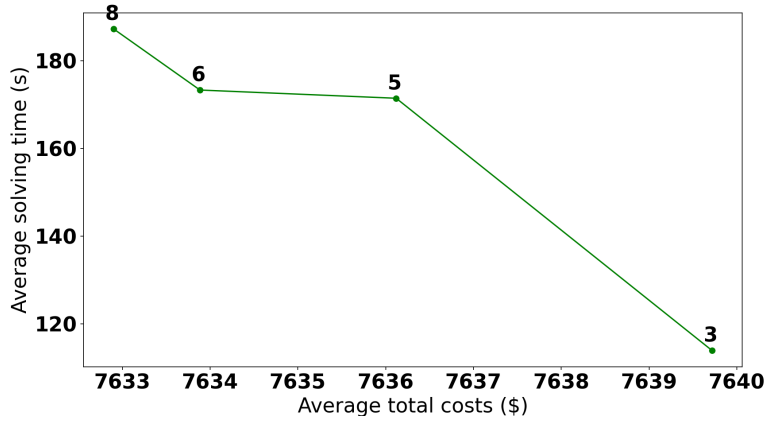

Figure 5. Resulting Pareto front for the Stage-2 MIP model on the training set with tested hyperparameter values. Each point represents a value of the number of points in the grid sampling used to approximate the energy consumption functions for the durations ($\tilde{t}$) that dominates either on average total costs or average solving time on the training set. This value is shown above each point in the plot. This Pareto front can then be used to choose the value of this hyperparameter to use on the test set (3).

The genetic algorithm has many hyperparameters. Since the algorithm runs for a given number of generations, the choice of hyperparameters mostly does not affect the computation time (except for the population size and the maximal number of generations). As a result, for this algorithm, we are interested in choosing hyperparameters that minimize the total costs only. However, testing a single combination of hyperparameters takes up to 30 minutes and the search space is large enough that we cannot effectively use a grid search. Instead, we use Bayesian optimization [29] to explore the search space and find a good combination of hyperparameters. The most important hyperparameters are the crossover

type, the mutation percentage, the population size, and the number of parents to keep between each generation. We determine the maximal number of generations in relation to the population size in order to have a total of 15,000 individuals, which corresponds to approximately five minutes of computation time for a medium-sized instance. We fixed the following hyperparameters: parent selection type: steady state selection; mutation type: random between -1 and 1. We also use early stopping when the best solution has not improved for 40 generations. The following state space (of size 30,560) is explored by the Bayesian optimization algorithm for 64 iterations, with the best combination found in bold:

- Crossover type: [Single Point or Two Points] (**Two Points**);
- Mutation percentage: 1 to 20 (**4**);
- Population size: 10 to 200 (**144**);
- Number of parents to keep: 2 to 5 (**2**).

4. Results and Discussions

The objective of the S-FRHACP-VS is to minimize total costs, thus this performance criterion will be used to evaluate each approach. However, the solving time will also be evaluated since it is a relevant criterion for the use of the approaches in the real world. Since the S-FRHACP-VS is a novel problem, no other work exists in the literature. As such, the new algorithms proposed in this paper, such as the genetic algorithms (*GA* and *GA-Warm-Start*) and the MIP heuristics (*ITS-MIP-H* and *ITS-MIP-H-One-It*) are compared to algorithms previously published for similar problems described in Section 2. Mainly, the Fuel-First Heuristic (*FF-H*) [13], the Max-Battery Heuristic (*MB-H*) [13], two dynamic programming heuristics (*DP* and *DP+GD*) [13] and a MIP model (*S1-MIP-H*) [14]. The main difference between our approaches and these approaches is that none of these approaches in the literature optimizes the flight speed.

Table 5 presents the solving time of each instance in seconds as well as total costs—distinguished between the minimum, maximum, and mean costs over 20 runs with a confidence interval of 95% for all approaches. *GA-Warm-Start* is the genetic algorithm that uses all non-MIP solutions as starting individuals, while *GA* is the genetic algorithm that starts from random individuals. All approaches except for the *GA-Warm-Start* and *GA* are deterministic, thus the same solution is obtained for each run and only this solution is presented. Moreover, for `TB`, the fuel cost does not vary, thus *DP+GD* returns the same solution as *DP*. *ITS-MIP-H-One-It* is the iterative two-stage MIP heuristic with one single iteration. Only *ITS-MIP-H*, *ITS-MIP-H-One-It*, *GA*, and *GA-Warm-Start* optimize speed, all other approaches use the recommended speed.

4.1. Total Costs

For total costs, *ITS-MIP-H* obtains the smallest costs for all instances, with an average of \$7,918.29. Figure 6 presents the average difference in total costs between the *ITS-MIP-H* and each other approaches, with a positive value representing that the *ITS-MIP-H* obtains solutions that are smaller/better. Figure 7 presents the average percentage increase in the total costs of all approaches over the test instances in comparison with the *ITS-MIP-H*. The iterative process allows on average the *ITS-MIP-H* to reduce the total cost by \$145 (2.33%), while reducing the total costs on average by \$578 (7.63%) compared to the best model that does not optimize the speed (*S1-MIP-H*). This shows the benefits of optimizing the speed on the total costs. In comparison with the *DP+GD*, the *ITS-MIP-H* reduces the total costs on average by \$700 (8.87%) and \$955 (11.43%) compared with the *DP*. *MB-H* greedily tries to maximize battery usage by always burning fuel first to minimize overall weight. It

Table 5. Solving time of each instance in seconds as well as total costs—distinguished between the minimum, maximum and mean costs over 20 runs with a confidence interval of 95% for the genetic algorithms (*GA* and *GA-Warm-Start*). Results reported for the Iterative Two-Stage MIP Heuristic (*ITS-MIP-H*), the ITS-MIP-H ran for a single iteration (*ITS-MIP-H-One-It*), the Stage-1 MIP model (*S1-MIP-H*), the genetic algorithms (*GA* and *GA-Warm-Start*), the Dynamic Programming approaches with and without the gradient descent post-treatment (*DP* and *DP+GD*), the Fuel-First Heuristic (*FF-H*), and the Max-Battery Heuristic (*MB-H*).

Instance	Approach	Solving Time (s)	Total Costs ($)		
			Mean	Min	Max
TB	*ITS-MIP-H*	8.47 ± 2.26	**4,053.79**		
	ITS-MIP-H-One-It	2.80 ± 0.67	4,273.82		
	S1-MIP-H	1.77 ± 0.37	4,638.25		
	GA-Warm-Start	192.08 ± 33.47	4,273.76 ± 54.25	4,221.96	4,343.96
	GA	190.00 ± 32.02	4,571.74 ± 460.19	4,232.65	5,036.84
	DP+GD	1.35 ± 0.45	4,691.55		
	DP	1.35 ± 0.45	4,691.55		
	MB-H	0.64 ± 0.45	5,018.40		
	FF-H	0.07 ± 0.02	5,050.80		
OT	*ITS-MIP-H*	8.88 ± 2.61	**5,698.82**		
	ITS-MIP-H-One-It	3.50 ± 0.91	6,037.98		
	S1-MIP-H	1.75 ± 0.45	6,380.47		
	GA-Warm-Start	178.84 ± 29.56	6,069.29 ± 160.81	5,925.75	6,223.41
	GA	172.84 ± 29.59	6,351.04 ± 313.95	6,090.42	6,593.51
	DP+GD	4.70 ± 1.86	6,399.29		
	DP	1.44 ± 0.51	6,675.27		
	MB-H	0.78 ± 0.30	7,471.08		
	FF-H	0.08 ± 0.04	7,925.38		
KT	*ITS-MIP-H*	17.85 ± 4.32	**7,257.39**		
	ITS-MIP-H-One-It	6.13 ± 1.22	7,276.22		
	S1-MIP-H	4.36 ± 1.13	7,760.52		
	GA-Warm-Start	205.04 ± 33.27	7,562.22 ± 90.32	7,491.41	7,652.06
	GA	197.59 ± 33.63	7,753.63 ± 196.47	7,516.39	7,867.23
	DP+GD	4.66 ± 1.38	7,886.30		
	DP	1.62 ± 0.74	8,085.75		
	MB-H	1.27 ± 0.81	8,454.27		
	FF-H	0.10 ± 0.06	9,082.64		
ST	*ITS-MIP-H*	13.59 ± 3.36	**9,464.36**		
	ITS-MIP-H-One-It	8.71 ± 2.24	**9,464.36**		
	S1-MIP-H	2.36 ± 0.71	9,943.74		
	GA-Warm-Start	254.99 ± 40.33	9,626.34 ± 78.14	9,532.82	9,694.56
	GA	249.36 ± 41.44	9,737.01 ± 246.42	9,584.15	9,999.04
	DP+GD	3.37 ± 0.92	10,051.21		
	DP	1.74 ± 0.67	10,609.48		
	MB-H	1.86 ± 0.81	10,844.11		
	FF-H	0.10 ± 0.03	11,184.57		
TV	*ITS-MIP-H*	19.24 ± 4.51	**12,264.88**		
	ITS-MIP-H-One-It	7.03 ± 1.62	12,386.53		
	S1-MIP-H	3.10 ± 0.63	12,882.24		
	GA-Warm-Start	322.62 ± 53.64	12,605.92 ± 42.12	12,583.10	12,654.47
	GA	315.12 ± 47.48	12,874.55 ± 199.33	12,708.59	13,024.28
	DP+GD	3.37 ± 1.10	12,943.05		
	DP	2.44 ± 1.15	13,111.35		
	MB-H	2.97 ± 1.01	13,449.69		
	FF-H	0.16 ± 0.11	13,931.27		
VT	*ITS-MIP-H*	12.29 ± 3.25	**8,770.51**		
	ITS-MIP-H-One-It	4.08 ± 1.21	8,945.93		
	S1-MIP-H	1.55 ± 0.67	9,371.25		
	GA-Warm-Start	250.40 ± 30.76	9,407.06 ± 119.86	9,294.66	9,544.14
	GA	241.74 ± 20.87	9,295.94 ± 416.15	8,909.14	9,666.08
	DP+GD	4.06 ± 1.64	9,874.05		
	DP	1.59 ± 0.41	10,063.71		
	MB-H	1.56 ± 0.78	10,268.48		
	FF-H	0.08 ± 0.03	10,511.44		

performs significantly worse than the other approaches with an average $1,333 (15.54%) difference with *ITS-MIP-H*. *FF-H* is a heuristic that does not use electricity except when

mandatory. This heuristic is a good comparison point to evaluate the potential benefits of using hybrid electric aircraft. For all instances it has the highest cost, with an average reduction of \$1,696 (18.64%) compared with the *ITS-MIP-H*. This shows that considering a hybrid electric engine for an aircraft could lead to reduction of 18% in the operating cost of a company. Moreover, this reduction is smaller when using only the recommended speed, \$1,118 (11.95%). Thus, varying the speed allows to reduce further the operating costs by 6.69% compared with *FF-H*.

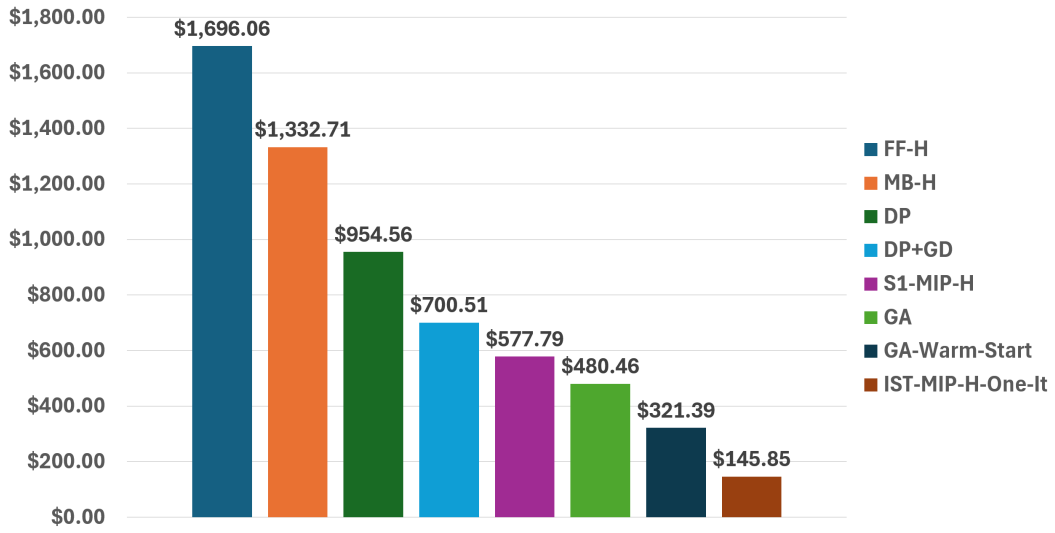

Figure 6. Average increase in total costs over the test instances of each approach in comparison with the *ITS-MIP-H* approach.

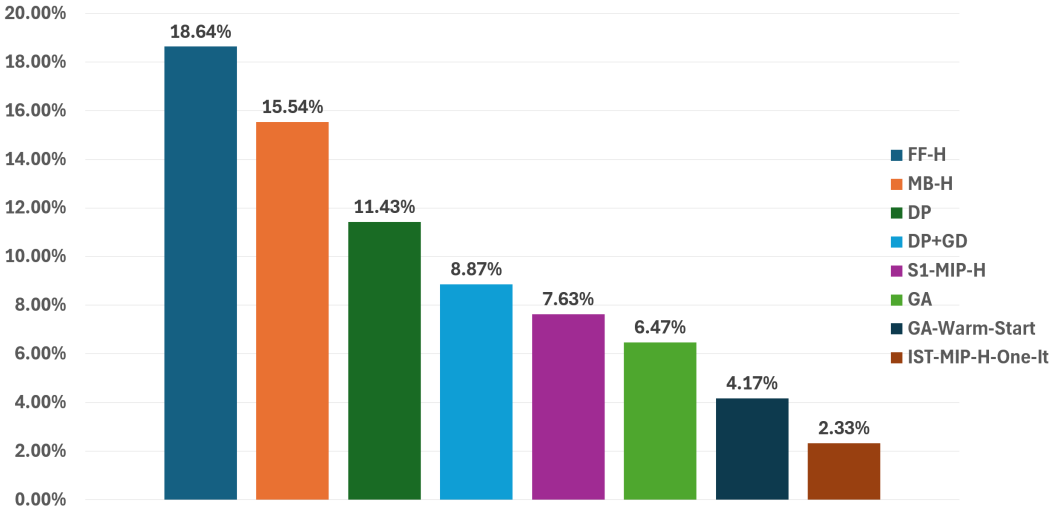

Figure 7. Average percentage increase in total costs over the test instances of each approach in comparison with the *ITS-MIP-H* approach.

For the *GA-Warm-Start* and *GA*, we compare by computing an average over the 20 runs to obtain an estimate of the performance of the algorithms on average. We observe that both approaches yield higher total costs for all instances in comparison with the *ITS-MIP-H* with an average augmentation of \$480 (6.46%) compared with *GA* and \$321 (4.17%) in comparison with *GA-Warm-Start*. Moreover, the size of the confidence interval for *GA* is much larger than *GA-Warm-Start*, suggesting that injecting solutions of all non-MIP solutions helps to obtain a better solution more frequently. Except for `VT`, usage of the warm

start allows to obtain better solutions, both in the best case and on average. The solutions obtained without warm start are similar to the solutions obtained without optimizing speed (*DP+GD* and *S1-MIP-H*). Compared to the best model that does not optimize speed (*S1-MIP-H*), *GA-Warm-Start* reduces total costs on average by \$239 (3.56%), while *GA* reduces total costs by \$65 (0.83%).

4.2. Solving Time

Figure 8 presents the average solving time of all approaches over the test instances. All approaches, except genetic algorithms, solve all instances in less than 20 seconds. *ITS-MIP-H* has the highest solving time of these approaches, with an average of 13.4 seconds to compute its solution. It is on average 5.64 times slower than *S1-MIP-H*, showing that considering the speed makes the problem significantly harder to solve. A single iteration of the iterative two-stage MIP heuristic on average doubles the solving time, suggesting that the Stage-2 MIP model has a similar complexity than the Stage-1 MIP model. Finally, genetic algorithms have, by far, the longest solving time. The maximal number of generations has been reached on all instances, suggesting that the genetic algorithms did not converge, assuming that the genetic algorithms have converged when the best solution has not changed after 40 consecutive iterations.

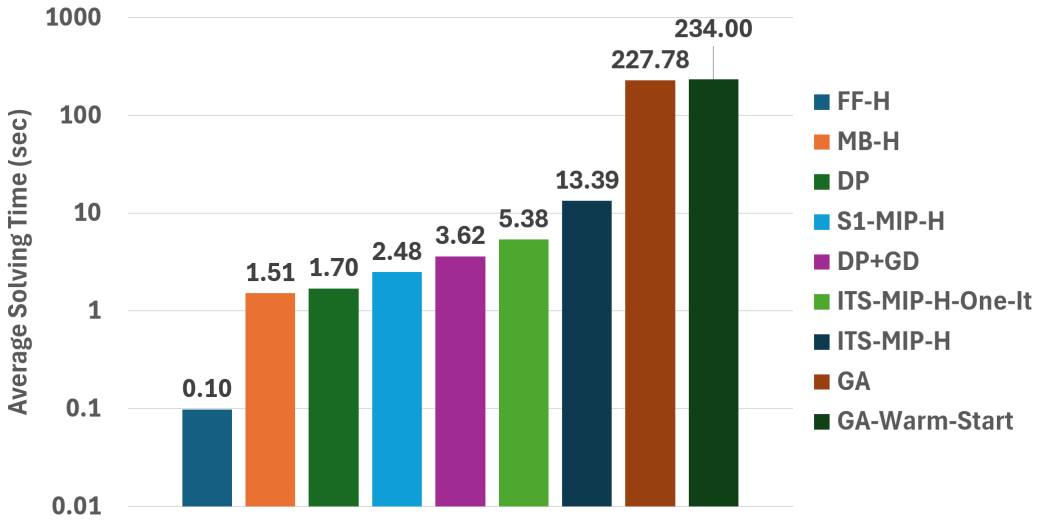

Figure 8. Semi log plot of the average solving time (sec) of each approach over the test instances.

4.3. Genetic Algorithms until Convergence

As a complementary experiment, the genetic algorithms (*GA* and *GA-Warm-Start*) were run until convergence on a single run to compare the returned solution after the limited number of generations and the converged solution. The behavior is expected to be similar for all runs. Figures 9 and 10 present a convergence plot of each algorithm for each instance. The dashed orange line represents the solution obtained after the generation limit of 105 generations (representing 15 000 individuals). We observe that the number of generations before convergence varies significantly between instances (from 300 to over 800 generations), while *GA-Warm-Start* reduces the number of generations needed for half of the instances (`KT`, `OT`, and `VT`). Figure 11 presents the solving time of the two genetic algorithms for each instance needed to reach convergence in comparison with the solving time after reaching the maximal number of generations. Figure 12 presents the reduction in total costs obtained by running the genetic algorithms until convergence for each instance. The solving time increases on average to approximately 1,000 seconds per instance for both

genetic algorithms, with total costs reduced by \$192 for *GA* and \$118 for *GA-Warm-Start* compared to the value from Table 5. For all instances, the converged solution always has higher total costs than the *ITS-MIP-H*, meaning that the *ITS-MIP-H* is still the best approach in terms of solving time and total costs.

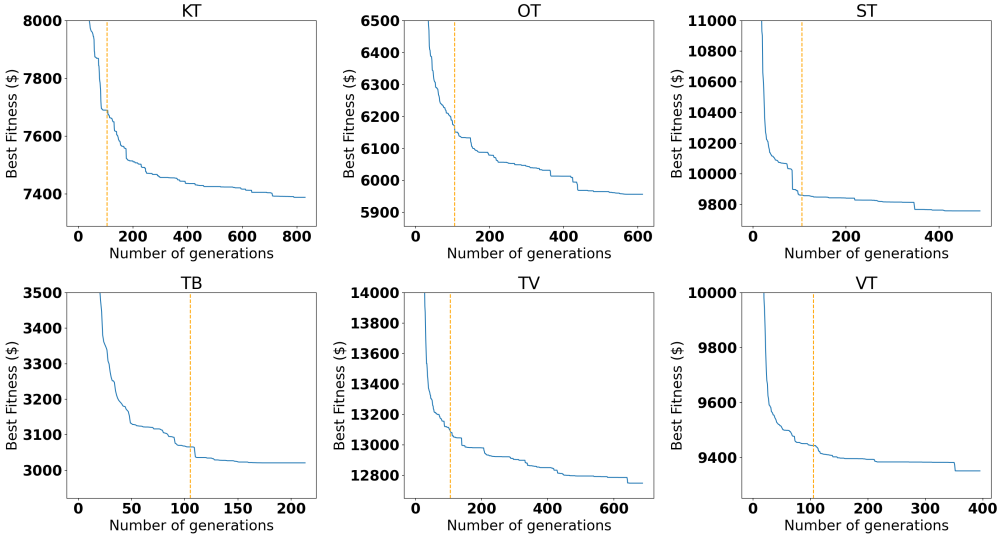

Figure 9. Convergence plot of the *GA* approach for each instance. The dashed orange line represents the best solution obtained at the generation limit (15 000 individuals, which represents 105 generations). The Y axis has been cropped, since the first generations have high value best individuals.

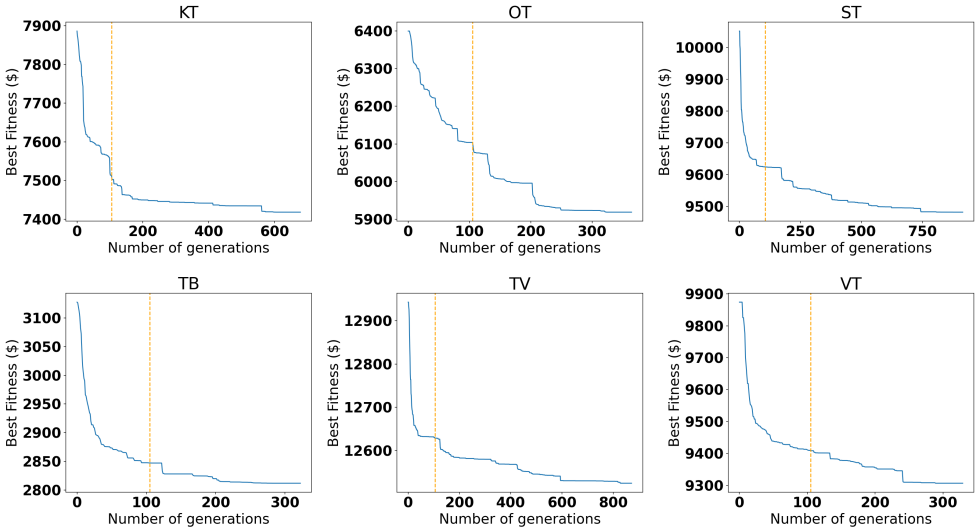

Figure 10. Convergence plot of the *GA-Warm-Start* approach for each instance. The dashed orange line represents the best solution obtained at the generation limit (15 000 individuals, which represents 105 generations).

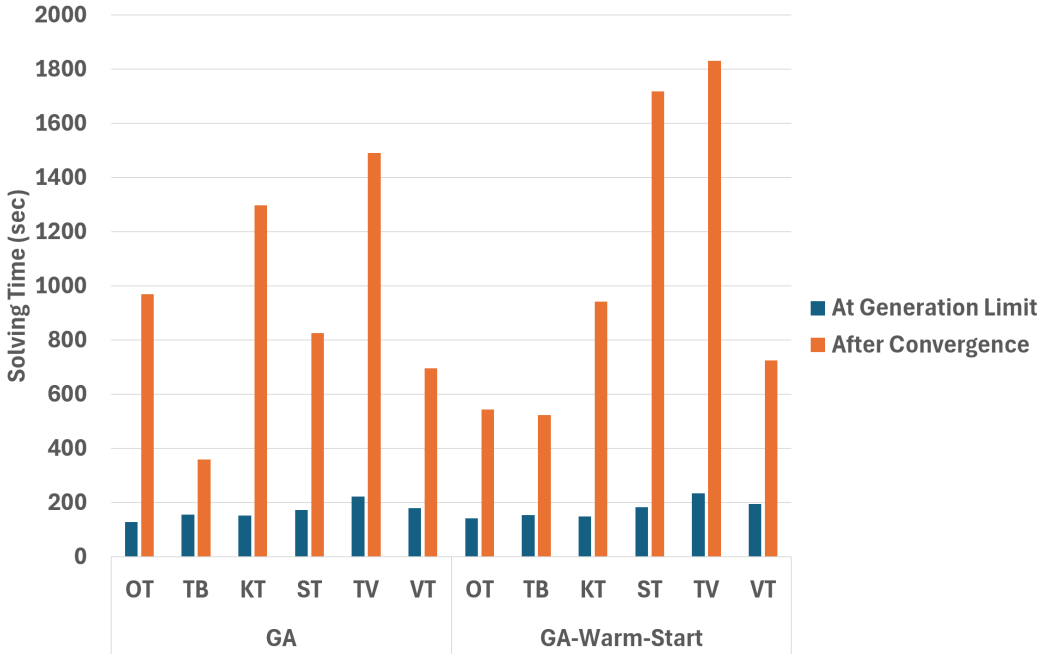

Figure 11. Solving time (sec) of the genetic algorithms with and without warm start for each instance at generation limit (15 000 individuals) and after convergence (40 consecutive generations without improvements).

Figure 12. Difference in total costs between the solution of each genetic algorithm between the solution obtained after convergence (40 consecutive generations without improvements) and the solution obtained at generation limit (15 000 individuals) for each instance.

4.4. Genetic Algorithm with MIP Warm Start

We also explored the potential of using the MIP solutions (*S1-MIP-H*, *ITS-MIP-H-One-It*, and *ITS-MIP-H*) as warm start solutions for the genetic algorithm. Figure 13 presents the difference in total costs between the genetic algorithm using MIP solutions as warm start and the *ITS-MIP-H* solution. On average, the genetic algorithm improves all solutions with

an average reduction of \$4.56 in comparison to the *ITS-MIP-H* with a maximum of \$12.53 for TB and a minimum of \$0.37 for KT. Thus, at best, it is able to improve the solutions by removing approximation errors from the linearization of the energy consumption functions, but these improvements are marginal, and the genetic algorithm does not seem to be able to further improve the solutions returned by the *ITS-MIP-H*.

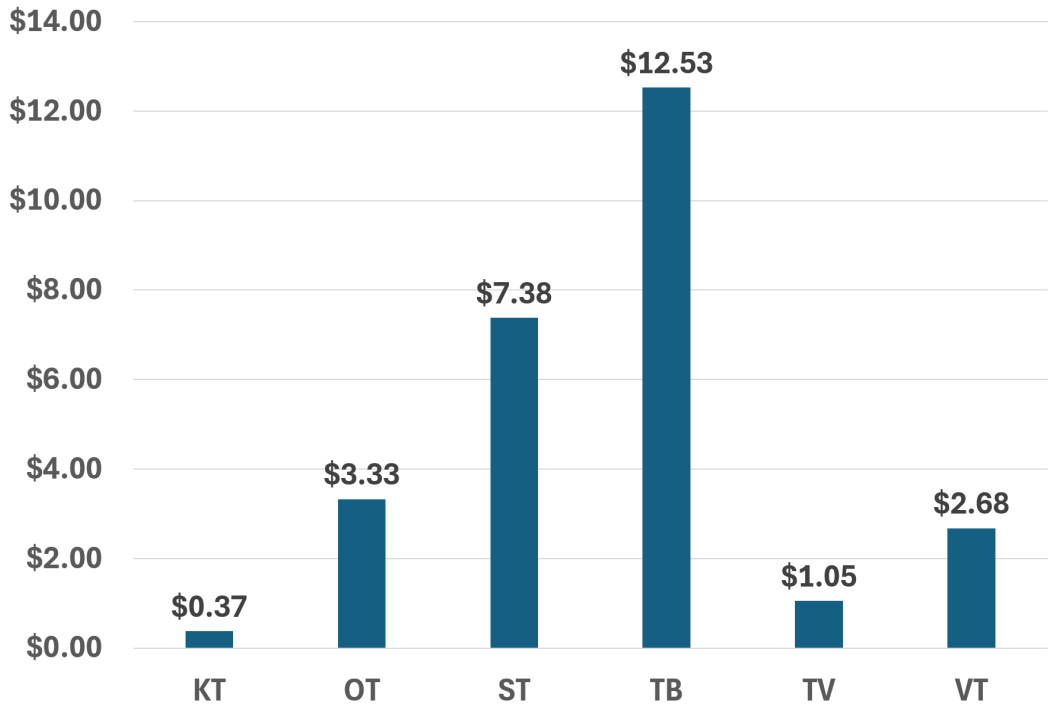

Figure 13. Difference in total costs between the solution of the genetic algorithm that uses MIP solutions as warm start and the solution obtained by *ITS-MIP-H* for each instance.

5. Conclusions

In this paper, we present the Soft Fixed Route Hybrid Electric Aircraft Charging Problem with Variable Speed (S-FRHACP-VS), a generalization of the S-FRHACP where flight speed decisions are considered. We showed that considering flight speed decisions makes the problem significantly harder to solve with known Mixed-Integer Programming approaches. We thus propose two new heuristics to solve it: 1) an iterative variable-based fixation heuristic (Iterative Two-Stage MIP Heuristic), and 2) genetic algorithms using other solutions (state of the art solution for previously published similar problems) as warm start. We compare our proposed models with previously published approaches to solve similar problems on the same benchmark proposed by Deschênes *et al.* [14] consisting of ten realistic instances representing real potential flights in Canada and France. These instances are published as a benchmark for this problem.

For all instances, the Iterative Two-Stage MIP Heuristic (*ITS-MIP-H*) performs better than all other approaches, including genetic algorithms. We showed that considering variable speed allows to reduce the average total cost by \$578 in comparison to the best approach from the literature that does not optimize speed. Moreover, considering hybrid electric aircraft instead of a fuel-only aircraft allows to reduce total costs on average by \$1,696 per flight compared to an approach that does not use the electric battery. However, the iterative process of the *ITS-MIP-H* does not guarantee convergence to a global optimum. Moreover, the results are highly dependent on the choice of hyperparameters for the size of the grid

used to linearize the energy consumption functions. In this paper, these hyperparameters are chosen using the energy consumption function of OpenAP [18], specialized for fuel consumption prediction and is not highly nonlinear. In the future, once real-world data will become available, advanced highly nonlinear machine learning models, such as neural networks, could be developed to more accurately predict the energy consumption. As a result, higher grid size might be necessary to approximate these functions and lead to significantly higher solving time.

In contrast, genetic algorithms do not suffer from this problem as they do not rely on approximation of the energy consumption functions. Moreover, they are easier to implement than the MIP models, thus, in practice, they could be interesting options for aircraft operators that do not have the resources to buy a CPLEX license and implement the Iterative Two-Stage MIP Heuristic. Implementing the linearizations for the charging function and energy consumption functions can indeed be tricky in comparison with using simple genetic algorithm known frameworks. However, on average, the genetic algorithms are outperformed by the *ITS-MIP-H* on total costs ($321) and solving time. Table 6 summarizes the key differences between the *ITS-MIP-H* and *GA-Warm-Start*, highlighting the advantages and disadvantages of each approach.

Table 6. Comparison of ITS-MIP-H vs. Genetic Algorithm for different criteria, mainly the total costs, solving time, ease of implementation, and the need for function approximation.

Criterion	ITS-MIP-H	GA (Warm Start)	Remarks
Total Costs	Best overall	Slightly higher costs	GA still competitive (avg +$321)
Solving Time	13 sec	230–320 sec	GA slower by 18–25×
Ease of Implementation	Complex (MIP, function linearization)	Simple (known frameworks)	GA is user-friendly and flexible
Function Approximation	Required (grid sampling approximations)	Not needed	GA supports black-box modeling

Injecting previous solutions as starting solutions generally helps improve the solution returned by the genetic algorithm by yielding better results with smaller variation between runs than without the warm start. In comparison with the best approach that does not optimize speed in the literature, the best genetic algorithm reduces total costs by $239 on average, suggesting that this algorithm is still interesting in practice.

These results provide new insights into the integration of hybrid electric aircraft within transportation networks, contributing to advancements in aircraft routing optimization, energy-efficient operations, and sustainable aviation policy development. For future work, generalizing this problem to a fleet of hybrid electric aircraft could be explored, as well as problem-specific mutations and crossovers to further enhance the performance of the genetic algorithm. Moreover, the gene encoding of the genetic algorithm could be used to explore other approaches such as gradient-descent based algorithms and blackbox optimization techniques.

Author Contributions: Conceptualization, Anthony Deschênes, Raphaël Boudreault, Jonathan Gaudreault and Claude-Guy Quimper; Data curation, Anthony Deschênes and Raphaël Boudreault; Formal analysis, Anthony Deschênes and Raphaël Boudreault; Funding acquisition, Anthony Deschênes, Raphaël Boudreault, Jonathan Gaudreault and Claude-Guy Quimper; Investigation, Anthony Deschênes and Raphaël Boudreault; Methodology, Anthony Deschênes, Raphaël Boudreault, Jonathan Gaudreault and Claude-Guy Quimper; Project administration, Raphaël Boudreault, Jonathan Gaudreault and Claude-Guy Quimper; Resources, Anthony Deschênes, Raphaël Boudreault, Jonathan Gaudreault and Claude-Guy Quimper; Software, Anthony Deschênes and Raphaël Boudreault; Supervision, Raphaël Boudreault, Jonathan Gaudreault and Claude-Guy Quimper; Validation, Anthony Deschênes, Raphaël Boudreault and Claude-Guy Quimper; Visualization, Anthony Deschênes; Writ-

ing – original draft, Anthony Deschênes; Writing – review & editing, Anthony Deschênes, Raphaël Boudreault and Claude-Guy Quimper. All authors have read and agreed to the published version of the manuscript.

Funding: This work received financial support from the Consortium for Research and Innovation in Aerospace in Quebec (CRIAQ), the Mitacs Accelerate program, the Natural Sciences and Engineering Research Council of Canada (CRSNG) and the *Fonds de recherche du Québec - Nature et technologie* (FRQNT).

Data Availability Statement: The dataset is available at https://github.com/AnthonyDeschenes/S-FRHACP-VS-Dataset

Acknowledgments: The authors would like to thank the many members of the Thales project team for their feedback on the problem definition and for the prototype implementation, especially Vanessa Simard for her contribution on the benchmark creation methodology.

Conflicts of Interest: Author Raphaël Boudreault was employed by the company Thales. The remaining authors declare that the research was conducted in the absence of any commercial or financial relationships that could be construed as a potential conflict of interest.

References

1. Cardone, L.; Petrone, G.; De Rosa, S.; Franco, F.; Greco, C. Review of the recent developments about the hybrid propelled aircraft. *Aerotecnica Missili & Spazio* **2024**, *103*, 17–37.
2. Bezos-O'Connor, G.M. NASA's Electrified Powertrain Flight Demonstration Project Overview. In Proceedings of the AIAA SciTech 2023, 2023.
3. Hagag, N.; Hoeveler, B. The feasibility of electric air taxis: balancing time-savings and co2 emissions-a joint case study of respective plans in Paris. *CEAS Aeronautical Journal* **2025**, pp. 1–26.
4. Ansell, P.J.; Haran, K.S. Electrified Airplanes: A Path to Zero-Emission Air Travel. *IEEE Electrification Magazine* **2020**, *8*, 18–26. https://doi.org/10.1109/MELE.2020.2985482.
5. Garrow, L.A.; German, B.; Schwab, N.T.; Patterson, M.D.; Mendonca, N.; Gawdiak, Y.O.; Murphy, J.R. A proposed taxonomy for advanced air mobility. In Proceedings of the AIAA Aviation 2022 Forum, 2022, p. 3321.
6. Straubinger, A.; Rothfeld, R.; Shamiyeh, M.; Büchter, K.D.; Kaiser, J.; Plötner, K.O. An overview of current research and developments in urban air mobility–Setting the scene for UAM introduction. *Journal of Air Transport Management* **2020**, *87*, 101852.
7. Long, Q.; Ma, J.; Jiang, F.; Webster, C.J. Demand analysis in urban air mobility: A literature review. *Journal of Air Transport Management* **2023**, *112*, 102436.
8. Moradi, N.; Wang, C.; Mafakheri, F. Urban Air Mobility for Last-Mile Transportation: A Review. *Vehicles* **2024**, *6*, 1383–1414. https://doi.org/10.3390/vehicles6030066.
9. Roy, S.; Maheshwari, A.; Crossley, W.A.; DeLaurentis, D.A. Future regional air mobility analysis using conventional, electric, and autonomous vehicles. *Journal of Air Transportation* **2021**, *29*, 113–126.
10. Justin, C.Y.; Mavris, D.N. Regional air mobility market study. *International Council of the Aeronautical Sciences* **2022**.
11. Li, S.; Rodrigues, L. Optimal cruise airspeed for hybrid-electric and electric aircraft: Applications to air mobility. In Proceedings of the 2023 IEEE Conference on Control Technology and Applications (CCTA). IEEE, 2023, pp. 295–300.
12. Mazzeo, F.; Di Ilio, G. Fuel cell hybrid electric propulsion system for a lightweight helicopter: Design and performance analysis in urban air mobility scenario. *International Journal of Hydrogen Energy* **2024**, *50*, 891–907.
13. Deschênes, A.; Boudreault, R.; Simard, V.; Gaudreault, J.; Quimper, C.G. Dynamic Programming for the Fixed Route Hybrid Electric Aircraft Charging Problem. In Proceedings of the International Conference on Combinatorial Optimization and Applications. Springer, 2023, pp. 354–365.
14. Deschênes, A.; Boudreault, R.; Gaudreault, J.; Quimper, C.G. A Mixed-Integer Programming Approach for an Extended Fixed Route Hybrid Electric Aircraft Charging Problem. In Proceedings of the Proceedings of the 14th International Conference on Operations Research and Enterprise Systems - Volume 1: ICORES. INSTICC, SciTePress, 2025, pp. 22–31. https://doi.org/10.5220/0013103400003893.
15. Montoya, A.; Guéret, C.; Mendoza, J.E.; Villegas, J.G. The Electric Vehicle Routing Problem with Nonlinear Charging Function. *Transportation Research Part B: Methodological* **2017**, *103*, 87–110. https://doi.org/10.1016/j.trb.2017.02.004.
16. Ansarey, M.; Shariat Panahi, M.; Ziarati, H.; Mahjoob, M. Optimal Energy Management in a Dual-Storage Fuel-Cell Hybrid Vehicle Using Multi-Dimensional Dynamic Programming. *Journal of Power Sources* **2014**, *250*, 359–371. https://doi.org/10.1016/j.jpowsour.2013.10.145.

17. De Cauwer, C.; Verbeke, W.; Coosemans, T.; Faid, S.; Van Mierlo, J. A Data-Driven Method for Energy Consumption Prediction and Energy-Efficient Routing of Electric Vehicles in Real-World Conditions. *Energies* **2017**, *10*, 608. https://doi.org/10.3390/en10050608.
18. Sun, J.; Hoekstra, J.M.; Ellerbroek, J. OpenAP: An Open-Source Aircraft Performance Model for Air Transportation Studies and Simulations. *Aerospace* **2020**, *7*, 104. https://doi.org/10.3390/aerospace7080104.
19. Tostado-Véliz, M.; Arévalo, P.; Jurado, F. An optimization framework for planning wayside and on-board hybrid storage systems for tramway applications. *Journal of Energy Storage* **2021**, *43*, 103207.
20. Pinto Leite, J.P.S.; Voskuijl, M. Optimal Energy Management for Hybrid-Electric Aircraft. *Aircraft Engineering and Aerospace Technology* **2020**, *92*, 851–861. https://doi.org/10.1108/AEAT-03-2019-0046.
21. Misener, R.; Floudas, C.A. Piecewise-Linear Approximations of Multidimensional Functions. *Journal of Optimization Theory and Applications* **2010**, *145*, 120–147. https://doi.org/10.1007/s10957-009-9626-0.
22. Wilbaut, C.; Salhi, S.; Hanafi, S. An iterative variable-based fixation heuristic for the 0-1 multidimensional knapsack problem. *European Journal of Operational Research* **2009**, *199*, 339–348.
23. Deschênes, A.; Gaudreault, J.; Vignault, L.P.; Bernard, F.; Quimper, C.G. The Fixed Route Electric Vehicle Charging Problem with nonlinear energy management and variable vehicle speed. In Proceedings of the 2020 IEEE International Conference on Systems, Man, and Cybernetics (SMC), 2020, pp. 1451–1458. ISSN: 2577-1655, https://doi.org/10.1109/SMC42975.2020.9283062.
24. Shami, T.M.; El-Saleh, A.A.; Alswaitti, M.; Al-Tashi, Q.; Summakieh, M.A.; Mirjalili, S. Particle swarm optimization: A comprehensive survey. *Ieee Access* **2022**, *10*, 10031–10061.
25. Nethercote, N.; Stuckey, P.J.; Becket, R.; Brand, S.; Duck, G.J.; Tack, G. MiniZinc: Towards a Standard CP Modelling Language. In Proceedings of the Principles and Practice of Constraint Programming – CP 2007; Bessière, C., Ed., Berlin, Heidelberg, 2007; Lecture Notes in Computer Science, pp. 529–543. Website: https://www.minizinc.org/, https://doi.org/10.1007/978-3-540-74970-7_38.
26. Gad, A.F. Pygad: An intuitive genetic algorithm python library. *Multimedia tools and applications* **2024**, *83*, 58029–58042.
27. Brent, R.P. *Algorithms for minimization without derivatives*; Courier Corporation, 2013.
28. Ehrgott, M.; Tenfelde-Podehl, D. Computation of Ideal and Nadir Values and Implications for Their Use in MCDM Methods. *European Journal of Operational Research* **2003**, *151*, 119–139. https://doi.org/10.1016/S0377-2217(02)00595-7.
29. Wu, J.; Chen, X.Y.; Zhang, H.; Xiong, L.D.; Lei, H.; Deng, S.H. Hyperparameter optimization for machine learning models based on Bayesian optimization. *Journal of Electronic Science and Technology* **2019**, *17*, 26–40.